



· 专题论著 ·



张波，中日友好医院超声医学科主任，主任医师，教授，博士研究生导师。中国医师协会超声医师分会浅表超声专业委员会副主任委员，中国临床肿瘤学会甲状腺癌专家委员会副主任委员，北京市抗癌协会甲状腺专业委员会副主任委员，北京女医师协会超声医学专业委员会指导专家、副主任委员，中华医学会北京医学会超声医学分会浅表器官与外周血管超声学组委员。擅长领域：甲状腺疾病的超声诊疗及新技术应用。研究成果：主持国家自然科学基金、北京市自然科学基金、清华大学“211工程”建设项目等17项。以第一作者或通信作者发表相关领域文章70余篇，其中在SCI收录期刊上发表20篇。执笔中英文指南与共识9篇。获2021年度中国研究型医院学会医学研究创新奖一等奖1项，2021年度华夏医学科技奖二等奖1项。2020年获评国之名医之“青年新锐”。

儿童及青少年甲状腺结节分级诊断模型的建立与验证

刘佳^{1,2}，李广涵³，高璐滢²，张紫杰¹，王莹²，熊颖¹，张波³

1. 民航总医院超声医学科，北京 100123；

2. 中国医学科学院北京协和医学院北京协和医院超声医学科，北京 100730；

3. 中日友好医院超声医学科，北京 100029

[摘要] 背景与目的：儿童及青少年甲状腺癌发病率逐年升高，且有较高的转移率及复发率。如果对儿童应用基于成人特点建立的甲状腺结节诊断标准则往往具有较高的漏诊率、误诊率和不必要活检率，本研究旨在建立儿童及青少年甲状腺结节的声像图分级诊断模型，对比其与美国放射学会（American College of Radiology, ACR）甲状腺影像报告与数据系统（Thyroid Imaging-Reporting and Data System, TI-RADS）的诊断效能。方法：纳入2000年1月—2017年10月中国医学科学院北京协和医学院北京协和医院收治的144例0~18岁的甲状腺结节患者作为训练集，2015年11月—2022年1月中日友好医院和民航总医院收治的41例0~18岁的甲状腺结节患者作为测试集，以病理学诊断作为金标准，将差异有统计学意义的超声特征进行多因素二元logistic回归分析，建立超声分级诊断模型并将模型带入测试集，比较其与ACR TI-RADS的诊断效能。结果：训练集中实性、低回声、纵横比 ≥ 1 、边缘不规则及微钙化等差异均有统计学意义（ $P < 0.05$ ）。Logistic回归分析显示，低回声、实性、边缘不规则及有钙化是诊断儿童及青少年甲状腺癌的独立预测因子。以上述独立预测因子建立超声分级系统，测试集中此分级模型与ACR TI-RADS相比具有更高的诊断准确率（92.7% vs 82.9%）。结论：以实性、低回声、边缘不规则及微钙化建立的分级诊断模型可用于儿童及青少年甲状腺结节的诊断，与ACR TI-RADS相比，具有更高的诊断准确率。

[关键词] 甲状腺癌；儿童；青少年；超声；分级诊断模型

DOI: 10.19401/j.cnki.1007-3639.2022.05.004

中图分类号: R736.1 文献标志码: A 文章编号: 1007-3639(2022)05-0397-07

第一作者: 刘佳 (ORCID: 0000-0002-6934-6179), 硕士, 住院医师 E-mail: 513726951@qq.com

通信作者: 张波 (ORCID: 0000-0003-0632-8333), 博士, 主任医师、教授, 中日友好医院超声医学科主任 E-mail: thyroidus@163.com

Establishment and test of graded diagnostic model of thyroid cancer in children and adolescents LIU Jia^{1,2}, LI Guanghan³, GAO Luying², ZHANG Zijie¹, WANG Ying², XIONG Ying¹, ZHANG Bo³ (1. Department of Ultrasound, Civil Aviation General Hospital, Beijing 100123, China; 2. Department of Ultrasound, Peking Union Medical College Hospital, Chinese Academy of Medical Sciences and Peking Union Medical College, Beijing 100730, China; 3. Department of Ultrasound, China-Japan Friendship Hospital, Beijing 100029, China)

Corresponding author: ZHANG Bo E-mail: thyroldus@163.com

[Abstract] Background and Purpose: The incidence rate of thyroid cancer in children and adolescents is increasing year by year, and there is a high rate of metastasis and recurrence. The application of diagnostic criteria for thyroid nodules based on adult characteristics in children has a high rate of missed diagnosis rate, misdiagnosis rate and unnecessary biopsy. This study aimed to establish a graded diagnostic model of thyroid nodules in children and adolescents, and to compare its diagnostic efficacy with American College of Radiology (ACR) Thyroid Imaging Reporting and Data System (TI-RADS). **Methods:** One Hundred and forty-four patients with thyroid nodules aged 0-18 years in Peking Union Medical College Hospital, Chinese Academy of Medical Sciences and Peking Union Medical College from January 2000 to October 2017 were included as the training set, and 41 patients with thyroid nodules aged 0-18 years in China-Japan Friendship Hospital and Civil Aviation General Hospital from November 2015 to January 2022 were included as the testing set. Taking pathological diagnosis as the gold standard, the statistically significant ultrasonic characteristics were analyzed by multivariate binary logistic regression. The ultrasonic grading diagnostic model was established and brought into the testing set to compare its diagnostic efficiency with ACR TI-RADS. **Results:** There was significant difference in solidity, hypoechoic, taller-than-wide shape, irregular edge and microcalcification between the two groups ($P < 0.05$). Logistic regression analysis showed that hypoechoic, solidity, irregular margin and calcification were independent predictors for the diagnosis of thyroid cancer in children and adolescents. When the ultrasonic grade was established based on the above independent predictors, this graded model had higher diagnostic accuracy in the testing set compared with ACR TI-RADS (92.7% vs 82.9%). **Conclusion:** The graded diagnostic model based on solidity, hypoechoic, irregular margin and microcalcification can be used in the diagnosis of thyroid nodules in children and adolescents. Compared with ACR TI-RADS, it has higher diagnostic accuracy.

[Key words] Thyroid cancer; Children; Adolescents; Ultrasound; Graded diagnostic model

甲状腺癌是儿童及青少年最常见的内分泌系统恶性肿瘤, 约占所有儿童及青少年癌症的11%^[1], 目前发病率为0.44/10万^[2], 且发病率逐年升高, 首都医科大学附属北京儿童医院的数据^[3]显示, 2006—2017年甲状腺癌住院手术患儿数量提高3倍以上。儿童及青少年甲状腺癌的生物行为亦与成人甲状腺癌不同, 发生转移及复发的概率更高, 转移率高达40%~80%, 复发率约30%^[4]。因此儿童及青少年甲状腺癌的早期诊断和治疗非常重要。

超声检查是甲状腺结节诊断的首选检查方法, 然而目前的诊断标准如2015年美国甲状腺学会(American Thyroid Association, ATA)指南^[5]及2017年美国放射学会(American College of Radiology, ACR)提出的甲状腺影像报告与数据系统(Thyroid Imaging-Reporting and Data System, TI-RADS)^[6]等, 均是基于成人的甲状腺超声特征建立。之前多项研究^[7-10]显示,

如果对儿童应用上述分级方法则往往具有较高的漏诊率、误诊率和不必要活检率。本研究旨在通过研究儿童及青少年甲状腺癌的超声特征, 试图建立一个适合儿童及青少年甲状腺结节的分级标准, 以更简单、有效地评估儿童及青少年的甲状腺结节。

1 资料和方法

1.1 资料

依据2015年ATA指南^[5]中儿童及青少年的定义(即 ≤ 18 岁), 训练集选取2000年1月—2017年10月在中国医学科学院北京协和医学院北京协和医院行甲状腺手术的144例0~18岁患者的176个结节, 测试集选取2015年11月—2022年1月中日友好医院及民航总医院收治的41例0~18岁患者的41个结节, 以上结节均以手术或穿刺标本的病理学诊断结果作为良恶性鉴别的金标准。

1.2 仪器和方法

1.2.1 仪器

采用美国GE公司Logiq 9和荷兰Philips公司iU 22等彩色多普勒超声诊断仪,高频线阵探头,频率5~14 MHz。

1.2.2 超声图像评估方法

采用盲法,由具有5年以上超声诊断经验的医师对超声图像进行回顾性研究。记录结节的超声特征(结构、纵横比、边缘、回声及钙化等)并依据ACR TI-RADS^[6]分级。

1.3 统计学处理

采用SPSS 25.0软件对数据进行分析。定量数据组间差异的比较,符合正态分布者采用 t 检验,不符合正态分布者采用非参数检验;计数资料组间差异的比较采用 χ^2 检验, $P < 0.05$ 为差异有统计学意义。以差异有统计学意义的超声特征为自变量,进行多因素二元logistic回归分析。利用受试者工作特征(receiver operating characteristic, ROC)曲线计算截断值和曲线下面积,计算其灵敏度、特异度、阳性预测值

(positive predictive value, PPV)、阴性预测值(negative predictive value, NPV)和准确率。

2 结果

2.1 临床特征

训练集176个结节中,良性结节63个(结节性甲状腺肿48个、炎性病变3个、腺瘤10个、甲亢治疗后改变2个),恶性结节113个(甲状腺乳头状癌106个、甲状腺滤泡癌6个、低分化癌1个)。两组间比较,年龄、结节个数及是否合并腺体弥漫性病变的差异无统计学意义($P > 0.05$),性别、结节大小区间分布的差异有统计学意义($P < 0.05$),恶性结节中95.7%的患者出现了颈部转移。测试集41个结节中,良性结节15个,恶性结节26个(1个结节为甲状腺滤泡癌,其余为甲状腺乳头状癌),其中8个结节为穿刺标本的活组织病理学检查,33个结节为手术后病理学检查,测试集41例患者中,女性34例,男性7例,年龄9~18岁,中位年龄16岁(表1)。

表1 训练集儿童及青少年甲状腺结节的临床特征

Tab. 1 The clinical characteristics of thyroid nodules in children and adolescents in training set

Clinical characteristic	Pathological result		P value
	Benign (N=63)	Malignant (N=113)	
Age/year median (range)	16 (10-18)	16 (6-18)	0.885
Gender <i>n</i>			0.035
Male	7	28	
Female	43	66	
Number of nodules <i>n</i>			0.053
Single	22	57	
Multiple	28	34	
Diffuse calcification	0	3	
Diffuse glandular lesions <i>n</i> (%)			0.095
With	23 (36.5)	56 (49.6)	
Without	40 (63.5)	57 (50.4)	
Size <i>n</i> (%)			0.001
<1 cm	11 (17.5)	27 (23.9)	
1-2 cm	9 (14.3)	38 (33.6)	
2-3 cm	14 (22.2)	27 (23.9)	
>3 cm	29 (46.0)	21 (18.6)	

2.2 超声特征比较

两组间超声特征比较, 实性、低回声、纵横比 ≥ 1 、边缘不规则及微钙化差异均有统计学意义(表2, 图1~3)。

2.3 多因素logistic回归模型分析结果

通过logistic回归分析筛选出低回声、实性、边缘不规则、有钙化为儿童及青少年甲状腺癌

的独立预测因子。所建模型为: $\text{Logist}(P) = -2.873 + 1.782 \times \text{实性} + 1.414 \times \text{低回声} + 1.779 \times \text{不规则} + 3.051 \times \text{有钙化}$ (表3)。ROC曲线的曲线下面积为0.96(95% CI: 0.94~0.99, 图4)。选取最佳截断值为 ≥ 3 时, 训练集诊断的灵敏度为83.2%, 特异度为95.2%, PPV为96.9%, NPV为75.9%, 准确率为87.5%。

表2 训练集儿童及青少年甲状腺结节的声像图表现

Tab. 2 The training set Sonographic representation of thyroid nodules in children and adolescents

Ultrasonic characteristic	Pathological result		P value
	Benign (N=63)	Malignant (N=113)	
Composition			<0.010
Solid	18 (28.6)	101 (89.4)	
Mixed cystic	45 (71.4)	12 (10.6)	
Cystic	0 (0.0)	0 (0.0)	
Echogenicity			<0.010
Hyperechoic	15 (23.8)	4 (3.5)	
Isoechoic	35 (55.6)	16 (14.2)	
Hypoechoic	13 (20.6)	93 (82.3)	
Very hypoechoic	0 (0.0)	0 (0.0)	
Anechoic	0 (0.0)	0 (0.0)	
Margin			<0.010
Rule	57 (90.5)	18 (15.9)	
Irregular	6 (9.5)	95 (84.1)	
Calcification			<0.010
Microcalcification	0 (0.0)	83 (73.5)	
Other calcification	2 (3.2)	1 (0.9)	
None	61 (96.8)	29 (25.7)	
Shape			<0.026
Wider-than-tall	62 (98.4)	95 (84.1)	
Taller-than-wide	1 (1.6)	18 (15.9)	

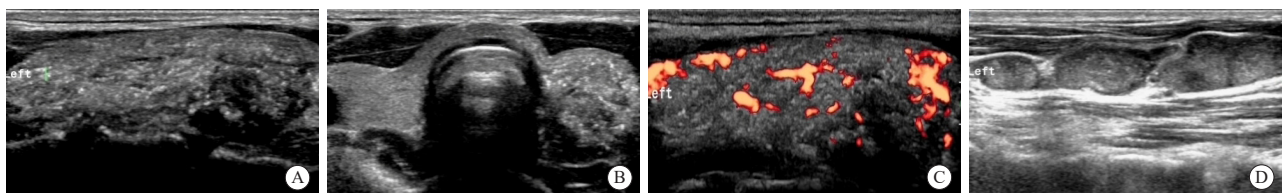


图1 男性, 18岁, 甲状腺乳头状癌

Fig. 1 Male, 18 years old, papillary thyroid carcinoma

A, B: Diffuse punctate calcification in the left lobe of thyroid gland. C: The distribution of blood flow signals in glands is irregular. D: Multiple abnormal lymph nodes were found in the left neck.

2.4 分级结果

训练集中，TI-RADS分级模型的截断值为5，分级模型中当截断值为高危时，前者具有较高的特异度、PPV，后者具有较高的灵敏度、NPV、准确率和约登指数，测试集中亦呈现类似的诊断表现（表4）。

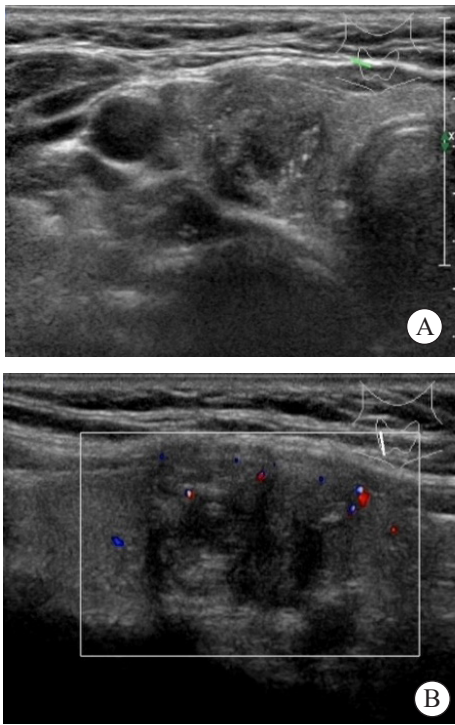


图2 女性，18岁，甲状腺右叶乳头状癌

Fig. 2 Female, 18 years old, papillary carcinoma of the right lobe of the thyroid gland

A: The right lobe of thyroid gland is hypoechoic, with irregular edges, local extension outside the capsule, and multiple punctate strong echoes inside. B: Punctate blood flow signals can be seen in the nodules.

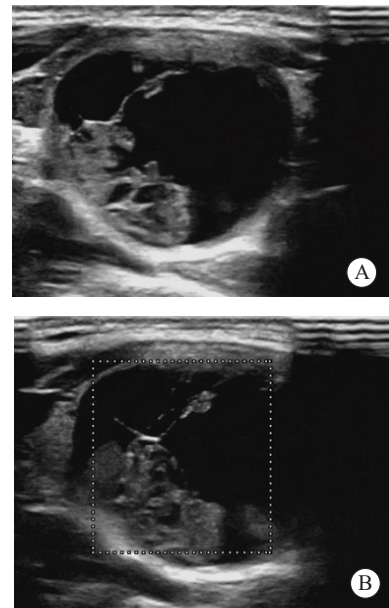


图3 男性，16岁，结节性甲状腺肿

Fig. 3 Male, 16 years old, nodular goiter

A: Cystic solid nodule in the left lobe of thyroid, with regular margin. B: No obvious blood flow signal was found in the nodule.

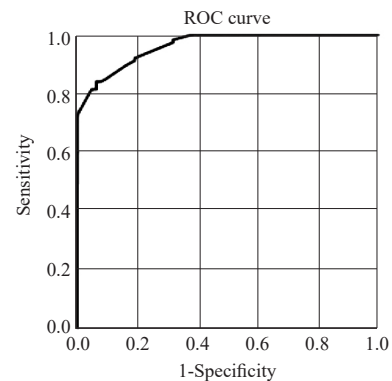


图4 二元logistic回归的ROC曲线

Fig. 4 ROC curve of binary logistic regression

表3 儿童及青少年甲状腺结节恶性风险的二元logistic回归分析

Tab. 3 Binary logistic regression analysis of malignant risk of thyroid nodules in children and adolescents

Independent variable	Partial regression coefficient	Standard error	Wals	P value	OR	95% CI
Composition (solid)	1.782	0.594	8.987	0.003	5.942	1.853-19.05
Echogenicity (hypoechoic)	1.414	0.612	5.333	0.021	4.113	1.239-13.66
Margin (irregular)	1.779	0.669	7.067	0.008	5.924	1.596-21.994
Calcification (with calcification)	3.051	0.905	11.356	0.001	21.129	3.584-124.579
Shape (taller-than-wide)	-0.842	1.252	0.452	0.501	0.431	0.037-5.015
Constant	-2.873	0.552	27.071	0.000	0.057	NA

NA: Not available.

表4 训练集及测试集ACR TI-RADS分级及分级诊断模型的诊断效能

Tab. 4 The diagnostic efficiency of ACR TI-RADS and graded diagnostic model in training set and testing set

Item	Sensitivity	Specificity	PPV	NPV	Accuracy	Jordan index
Training set						
ACR TI-RADS	75.2	96.8	97.7	68.5	83.0	0.72
The graded diagnostic model	83.2	95.2	96.9	75.9	87.5	0.78
Testing set						
ACR TI-RADS	73.1	100.0	100.0	68.2	82.9	0.73
The graded diagnostic model	96.2	86.7	92.6	92.9	92.7	0.83

3 讨 论

本研究纳入多中心数据研究儿童及青少年甲状腺癌的超声表现, 男性甲状腺癌的发病率低于女性, 恶性率高于女性, 与既往研究^[11-12]结果一致, 与成人相比, 儿童及青少年甲状腺癌更容易转移及复发^[4]。本研究中, 训练集的甲状腺癌患者转移率高达95.7%, 远高于成人(38.0%)^[13]。

单因素分析显示, 纵横比 ≥ 1 、低回声、实性、边缘不规则及微钙化对于鉴别甲状腺结节良恶性的差异有统计学意义。微钙化的特异度最高, 为100%, 且其检出率(73.5%)高于成人(67.9%~68.5%)^[14], 与Polat等^[15]的研究类似, 原因可能是儿童及青少年的细胞增殖速度较高, 新生血管生成速度相对较慢, 肿瘤局部血液供应不足, 细胞坏死后形成钙化层, 超声表现为微钙化^[16]。纵横比 ≥ 1 的特异度高(98.4%), 但灵敏度仅15.9%, 在多因素分析中被排除。Al Nofal等^[17]研究显示, 甲状腺癌的细胞增殖速度较高, 新生血管的生成速度相对较慢, 肿瘤局部血液供应受限, 纵横比 > 1 是一个罕见特征。但也有研究^[10]认为, 纵横比 > 1 有较高的诊断价值。另有研究^[18]发现, 在甲状腺长轴及短轴切面结节的纵横比均有较好的诊断价值, 但两者的最佳截断值不同。可能由于本研究为回顾性研究, 长轴及短轴切面均采用纵横比 ≥ 1 的标准, 从而使其灵敏度低, 整体诊断效率降低。本研究提示低回声具有较高的诊断效率, 与既往研究^[15]结论一致。实性结节为儿童及青少年甲状腺癌的独立预测因素, 但席雪华^[19]在成人的研

究中表明, 尽管实性结节与非实性结节的恶性率差异显著, 但实性仍不能作为一个独立指标来预测甲状腺癌的风险。因此, 对于实性在儿童及青少年甲状腺癌中的诊断效能还需要进一步大样本量的研究来验证, 且需结合其他的超声特征。几项指标中, 边缘不规则的准确率最高(86.4%), 特异度也较高(90.5%), 是甲状腺癌的独立预测因素, 这与Lim-Dunham等^[20]的研究结果一致。值得注意的是, 边缘不规则需要与边界不清相鉴别。边界不清可提示甲状腺结节的恶性风险, 但Park等^[21]研究显示, 边界不清的识别有较大的观察者间差异, 而且ACR TI-RADS也将边界不清归为0分, 故本研究未将边界不清纳入模型。

目前临床上常用的甲状腺结节分级标准为2015年ATA指南^[5]恶性风险分层及ACR TI-RADS^[6]分级, 虽有研究^[10]显示, 其在儿童及青少年甲状腺结节评估中有一定价值, 但儿童及青少年甲状腺结节的超声特征具有一定特殊性, 需要引起重视。本研究基于现有数据, 制定了儿童及青少年甲状腺结节良恶性诊断的超声分级标准, 将内部结构、回声、边缘及钙化4个独立因素分组, 有0项者为低危组, 有1~2项者为中危组, 有3~4项者为高危组, 具有较高的诊断准确率, 此外该分级相对比较简单, 易于学习与应用。

本研究的局限性在于作为回顾性研究, 选择的均为有明确病理学诊断的结节, 存在一定选择偏倚。其次, 由于儿童及青少年甲状腺结节的发病率低, 即使纳入多中心数据, 本研究的样本量依然较少。综上所述, 儿童及青少年甲状腺结节的临床特征及超声表现均与成人有所不同, 本研究建立的分级诊断模型可用于儿童及青少年甲状

腺结节的良恶性鉴别,与ACR TI-RADS相比,具有更高的诊断价值。

利益冲突声明:所有作者均声明不存在利益冲突。

[参 考 文 献]

- [1] SIEGEL R L, MILLER K D, JEMAL A. Cancer statistics, 2018 [J]. *CA A Cancer J Clin*, 2018, 68(1): 7-30.
- [2] 国家儿童医学中心, 国家儿童肿瘤监测中心, 中华医学会儿外科学分会, 等. 中国儿童甲状腺结节及分化型甲状腺癌专家共识 [J]. *中华实用儿科临床杂志*, 2020, 35(20): 1521-1530.
- National Center for Children's Health, National Children's Cancer Surveillance Center, Pediatric Surgery Branch of Chinese Medical Association, et al. Expert consensus on thyroid nodules and differentiated thyroid cancer for Chinese children [J]. *Chin J Appl Clin Pediatr*, 2020, 35(20): 1521-1530.
- [3] 王嘉丽, 任潇亚, 倪鑫, 等. 儿童甲状腺癌62例临床分析 [J]. *中华儿科杂志*, 2018, 56(8): 597-600.
- WANG J L, REN X Y, NI X, et al. Clinical analysis of thyroid cancer in 62 children [J]. *Chin J Pediatr*, 2018, 56(8): 597-600.
- [4] RIVKES S A, MAZZAFERRI E L, VERBURG F A, et al. The treatment of differentiated thyroid cancer in children: emphasis on surgical approach and radioactive iodine therapy [J]. *Endocr Rev*, 2011, 32(6): 798-826.
- [5] HAUGEN B R, ALEXANDER E K, BIBLE K C, et al. 2015 American Thyroid Association management guidelines for adult patients with thyroid nodules and differentiated thyroid cancer: the American Thyroid Association guidelines task force on thyroid nodules and differentiated thyroid cancer [J]. *Thyroid*, 2016, 26(1): 1-133.
- [6] TESSLER F N, MIDDLETON W D, GRANT E G, et al. ACR Thyroid Imaging, Reporting and Data System (TI-RADS): white paper of the ACR TI-RADS committee [J]. *J Am Coll Radiol*, 2017, 14(5): 587-595.
- [7] KIM P H, YOON H M, HWANG J, et al. Diagnostic performance of adult-based ATA and ACR TI-RADS ultrasound risk stratification systems in pediatric thyroid nodules: a systematic review and meta-analysis [J]. *Eur Radiol*, 2021, 31(10): 7450-7463.
- [8] PICCARDO A, FIZ F, BOTTONI G, et al. Facing thyroid nodules in paediatric patients previously treated with radiotherapy for non-thyroidal cancers: are adult ultrasound risk stratification systems reliable? [J]. *Cancers*, 2021, 13(18): 4692.
- [9] LIM-DUNHAM J E. Ultrasound guidelines for pediatric thyroid nodules: proceeding with caution [J]. *Pediatr Radiol*, 2019, 49(7): 851-853.
- [10] LIM-DUNHAM J E, TOSLAK I E, REITER M P, et al. Assessment of the American College of Radiology Thyroid Imaging Reporting and Data System for thyroid nodule malignancy risk stratification in a pediatric population [J]. *Am J Roentgenol*, 2019, 212(1): 188-194.
- [11] GUPTA A, LY S, CASTRONEVES L A, et al. A standardized assessment of thyroid nodules in children confirms higher cancer prevalence than in adults [J]. *J Clin Endocrinol Metab*, 2013, 98(8): 3238-3245.
- [12] DERMODY S, WALLS A, HARLEY E H Jr. Pediatric thyroid cancer: an update from the SEER database 2007-2012 [J]. *Int J Pediatr Otorhinolaryngol*, 2016, 89: 121-126.
- [13] LIU C X, XIAO C, CHEN J J, et al. Risk factor analysis for predicting cervical lymph node metastasis in papillary thyroid carcinoma: a study of 966 patients [J]. *BMC Cancer*, 2019, 19(1): 622.
- [14] LU Z H, MU Y M, ZHU H Q, et al. Clinical value of using ultrasound to assess calcification patterns in thyroid nodules [J]. *World J Surg*, 2011, 35(1): 122-127.
- [15] POLAT Y D, ÖZTÜRK V S, ERSOZ N, et al. Is thyroid imaging reporting and data system useful as an adult ultrasonographic malignancy risk stratification method in pediatric thyroid nodules? [J]. *J Med Ultrasound*, 2019, 27(3): 141-145.
- [16] 陈继来. 未成年人与成年人甲状腺癌超声特征差异性分析 [J]. *临床军医杂志*, 2018, 46(2): 221-223.
- CHEN J L. Analysis on the difference of ultrasonic characteristics between minors and adults with thyroid cancer [J]. *Clin J Med Off*, 2018, 46(2): 221-223.
- [17] AL NOFAL A, GIONFRIDDO M R, JAVED A, et al. Accuracy of thyroid nodule sonography for the detection of thyroid cancer in children: systematic review and meta-analysis [J]. *Clin Endocrinol (Oxf)*, 2016, 84(3): 423-430.
- [18] 付鹏, 陈文, 崔立刚, 等. 不同纵横比算法对预测甲状腺结节良恶性风险的价值 [J]. *中国医学科学院学报*, 2019, 41(5): 663-666.
- FU P, CHEN W, CUI L G, et al. Values of longitudinal and transverse plane ratios in predicting the risk of malignant thyroid nodules [J]. *Acta Acad Med Sin*, 2019, 41(5): 663-666.
- [19] 席雪华. 甲状腺结节超声多模态成像价值研究 [D]. 北京: 北京协和医学院, 2019.
- XI X H. Evaluated the value of ultrasonographic multimodality diagnostic model of thyroid nodules [D]. Beijing: Peking Union Medical College, 2019.
- [20] LIM-DUNHAM J E, ERDEM TOSLAK I, ALSABBAN K, et al. Ultrasound risk stratification for malignancy using the 2015 American Thyroid Association management guidelines for children with thyroid nodules and differentiated thyroid cancer [J]. *Pediatr Radiol*, 2017, 47(4): 429-436.
- [21] PARK C S, KIM S H, JUNG S L, et al. Observer variability in the sonographic evaluation of thyroid nodules [J]. *J Clin Ultrasound*, 2010, 38(6): 287-293.